



9th International Conference on Applied Energy, ICAE2017, 21-24 August 2017, Cardiff, UK

## The Performance of a 1.5 stage Axial Turbine with a Non-Axisymmetric Casing at Off-Design Conditions

Hakim T. K. Kadhim<sup>a,b</sup>, Aldo Rona<sup>a\*</sup>, Hayder M. B. Obaida<sup>a</sup>, and Katrin Leschke<sup>a</sup>

<sup>a</sup>University of Leicester, Leicester, LE1 7RH, U.K.

<sup>b</sup>Al-Furat Al-Awsat Technical University, Technical Institute, Al-Dewaniyah, Iraq

---

### Abstract

Advances in manufacturing techniques allow greater freedom in designing axial turbine stage passages, including non-axisymmetric end walls. A non-axisymmetric end wall design method for the stator casing is implemented through a novel surface definition, towards mitigating secondary flow losses. The new design is compared with a diffusion design from the literature. Off-design operations are considered. Numerical predictions of a 1.5 stage axial turbine show a reduction in the rotor row total pressure loss of 1.69 % against the benchmark axisymmetric stage from RTWH Aachen, which is validated against experiment. Flow analysis gives an insight into the effectiveness of the new surface definition approach, which is implemented using Alstom Process and Optimization Workbench (APOW) software at design conditions. The numerical predictions show that performance is retained at off-design conditions.

© 2017 The Authors. Published by Elsevier Ltd.

Peer-review under responsibility of the scientific committee of the 9th International Conference on Applied Energy.

*Keywords:* axial turbines; secondary flows; endwall modifications.

---

### 1. Introduction

The reduction of secondary flow losses is an active research area in turbomachinery, as these losses represent approximately 40% to 50% of the estimated total aerodynamic losses in an axial turbine [1]. Thus, reducing these

---

\* Corresponding author. Tel.: +44(0)116252 2510; fax: +44(0)116252 2525.

E-mail address: [ar45@leicester.ac.uk](mailto:ar45@leicester.ac.uk).

losses results in an increase in the turbine efficiency. Mitigating techniques for secondary flows related to the end wall are reviewed in Langston [2] and in Kadhim and Rona [3].

Langston [2] gives a review of the secondary flow structures that typically characterize an axial turbine stage, identified either by experiments or by Computational Fluid Dynamics (CFD), without considering tip clearance effects. Langston [2] identified three main vortices, namely the horseshoe vortex, the passage vortex and the corner vortex. These and other vortices are reported to be mutually interacting and difficult to separate from one another. The axial development and structure of these vortices, as reported in Wang et al. [4], are shown in Fig. 1(a). Sieverding [5] and Acharya and Mahmood [6] provided a detailed explanation of the flow features near the end wall that are caused by the interaction of the oncoming end-wall boundary layer with the blading. The upstream boundary layer bifurcates at the leading edge of the blade, forming a saddle point. Gostelow et al. [7] showed by flow visualization that a horseshoe vortex forms downstream of the saddle point and a sample of this visualisation is shown in Fig. 1(b).

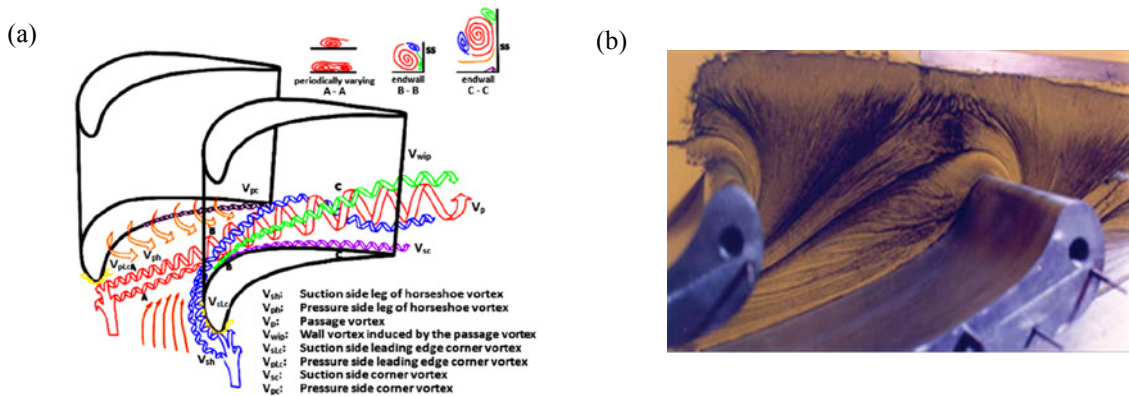


Fig. 1: (a) Secondary flows through a turbine blade passage [4], (b) visualisation of the horseshow vortex [7].

In this paper, three-dimensional steady RANS  $k-\omega$  SST and RNG  $k-\epsilon$  models of a 1.5 stage axial turbine with axisymmetric walls are validated against experimental measurements from the Institute of Jet Propulsion and Turbomachinery at the Rheinisch-Westfälische Technische Hochschule (RWTH) Aachen, Germany, using the OpenFOAM 3.2-extend solver. ANSYS ICEM CFD was used as the geometry and mesh generator. A non-axisymmetric casing design is then introduced based on a novel surface definition method that draws from observations of the typical secondary flow pattern over the casing.

## 2. CFD method

The Aachen turbine flow is investigated numerically by building a baseline three-dimensional steady RANS  $k-\omega$  SST model. OpenFOAM 3.2 extend with the steadyCompressibleMRFFoam solver generates the flow solutions using mixing planes at the stator–rotor interface. The computational domain is pitchwise periodic and one blade pitch around the annulus is modelled.

A simple H-mesh topology is applied to the first and second stators blades passages and an O-mesh topology is applied to the rotor blade passage. The rotor tip clearance is accounted for by adding an extra O-type block as shown in Fig. 4. This clustering provides a near-wall resolution of  $y^+ \approx 1$ . The turbine was tested with dry air as the working fluid under ideal gas conditions with constant specific heats. The specific heat ratio  $k = 1.4$ , the specific gas constant  $R = 287 \text{ J kg}^{-1} \text{ K}^{-1}$ , and the molecular viscosity is estimated by Sutherland's law. At the computational domain inflow, a fully developed inflow compressible boundary layer is imposed over the casing. This profile was generated by the EDDYBL program of Wilcox. At the outflow, a radial profile of static pressure is imposed, determined by radial equilibrium. Further details on the flow modelling, the test case, the computational mesh, and the boundary conditions are given in Kadhim et al. [8], [9].

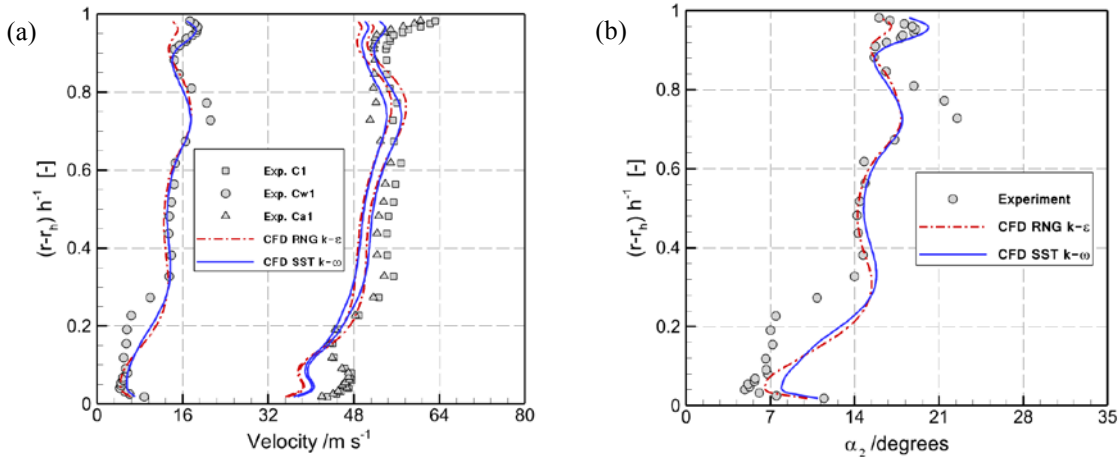


Fig. 2. Radial distributions of pitch mass-averaged (a) absolute (C1), axial (Ca1), and tangential (Cw1) velocity components and (b) yaw angle at 8.8 mm downstream of the rotor exit plane.

Fig. 2 (a) compares the radial profiles of pitch mass-averaged velocity components downstream of the rotor exit plane predicted by the RANS  $k-\omega$  SST and RNG  $k-\epsilon$  models against the measurements from RWTH Aachen. The velocity profiles are in broad agreement through the centre of the passage, whereas the tangential velocity component appears somewhat under-predicted near the hub. As this investigation is mainly concerned with the effect of the casing wall treatment, the agreement appears satisfactory for the purpose of the current work. Fig. 2 (b) shows a similar trend, with the numerical predictions giving up to 10 degrees of over-turning close to the hub and an overall better agreement with the measurements above 0.4 blade spans. The  $k-\omega$  SST turbulence closure appears to give predictions marginally closer to the measurements near the casing and therefore the predictions from this model are used in the remainder of this paper. This comparison adds to the model validation reports in Kadhim et al. [8] and provides confidence in the use of the numerical model for testing non-axisymmetric casing wall designs.

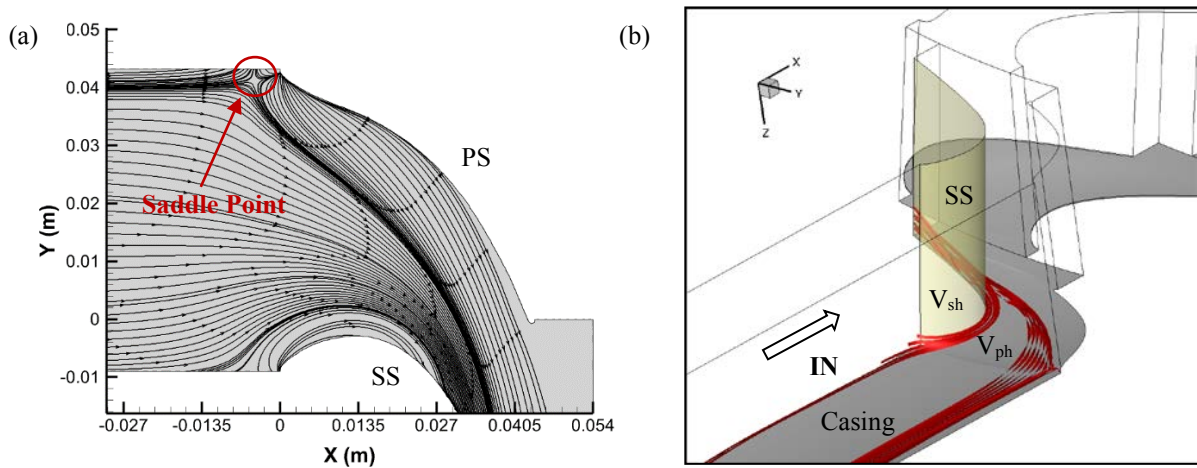


Fig. 3 (a) Flow visualization over the stator 1 axisymmetric casing showing the separation of oncoming casing boundary layer (saddle point) by the streamlines (b) The same surface showing by the ribbons the pressure side horseshoe vortex interacting with its suction side branch.

Fig. 3 (a) shows a numerical flow visualisation over the stator 1 axisymmetric casing by near-surface limit streamlines. This visualisation indicates the presence of the main flow structures outlined by Langston [2]. Specifically, the inflow to stator cascade blades features a growing boundary layer on the casing wall, along 143 mm

long passage leading edge. The upstream boundary layer bifurcates at the leading edge of the blade, forming a saddle point. The location of this bifurcation is highlighted by the arrow in Fig. 3 (a). Due to the interaction between the end wall boundary layer and the adverse pressure gradient from the blade potential pressure field, a horseshoe vortex is generated near the junction between the blade leading edge and the end wall. The horseshoe vortex left and right arms bend downstream into the passage on both pressure and suction sides as shown by ribbons in Fig. 3 (b). The bundle of ribbons towards the right edge of Fig. 3 (b) show that the pressure side arm of the horseshoe vortex moves across towards the suction side, under the influence of a pitchwise pressure gradient, merging with the suction side approximately 0.55 axial chords from the leading edge and creating a larger vortex structure, the passage vortex, as described by Langston [2]. The next section introduces a non-axisymmetric design of the stator casing to reduce the effect of these secondary flow features.

### 3. Non-axisymmetric Upstream Stator Casing Design

A non-axisymmetric casing design workflow has been implemented in the Alstom Process and Optimization Workbench (APOW) software. This workflow was executed in batch mode. A contoured casing surface generated in MATLAB and imported as NURBS in ANSYS ICEM CFD where computational domain is discretised. This was done maintaining similar meshing parameters to obtain the same mesh quality as for the validation test case given in Kadhim et al. [8]. The ANSYS ICEM CFD unstructured mesh was converted to OpenFOAM by the Fluent3DMeshToFoam pre-processor of OpenFOAM.

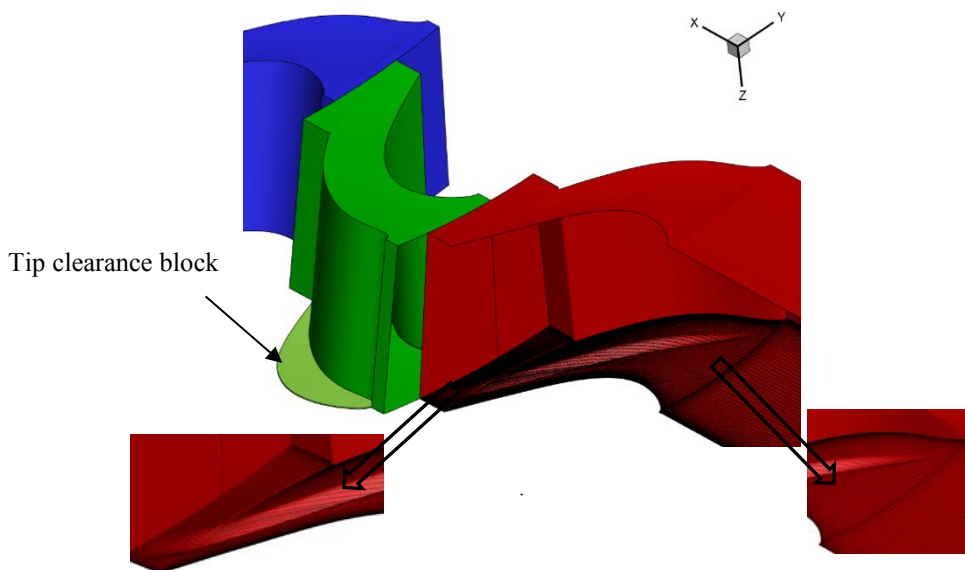


Fig. 4. Non-axisymmetric casing NURBS imported in ICEM CFD.

The casing wall is contoured by applying a groove to it, while the hub is kept axisymmetric. Two main variables were used in the parametrization of the non-axisymmetric turbine upstream stator casing: the maximum groove depth location along the groove path  $\mu(x, \theta_g)$  and the groove pitchwise width  $w(x, \theta_g)$ . The groove starts narrow at the stator leading edge and widens up to the stator exit. Figure 3 shows the casing with groove imported in ICEM CFD.

### 4. Results and Discussion

The validated simulation from section 2 was used as the baseline for studying the effects of contouring the casing, using Tecplot 2016 for post-processing. The same boundary conditions were applied as for the validation test case. The total pressure loss coefficient  $C_{pL}$ , evaluated across the stator and across the stage, was used to drive the non-

axisymmetric casing design. This was then tested numerically at off-design by reducing the rotor speed to 2510 r.p.m. This set point operation was reported by Gallus and Zeschky [10] as lowering the turbine isentropic efficiency, due to higher secondary flow losses. The new design was selected as the best design among four different configurations, by considering their loss, following the same approach used for design point operations by Kadhim et al. [9]. The selected design used a leading edge groove width of 12 mm. The groove width then widens monotonically up to the mixing plane (1) of Fig. 4 to twice its width at the leading edge. The maximum location of the groove depth is 65% of the total groove length. The new design provides a total pressure loss reduction of 1.69 % across the stage, compared to the baseline.

The diffusion surface design reported in Sun et al. [11] was used to compare the performance of the new end-wall design to the literature. This geometry was also tested at off-design. This design uses a cosinusoidal curve of half period in the circumferential direction to create a diffusing flow near the blade suction side, to increase the pressure locally and reduce the circumferential pressure gradient over the casing. A streamwise curve defines the amplitude of the cosinusoidal curve on different axial planes. This streamwise curve is defined as a non-uniform B-Spline with seven control points at seven prescribed axial positions. The first and the last points are fixed at the leading and trailing edge while the radial coordinate of the remaining five points is defined as in [11]. The design by [11] provides a total pressure loss reduction of 3.6 % across the stage, compared to the baseline.

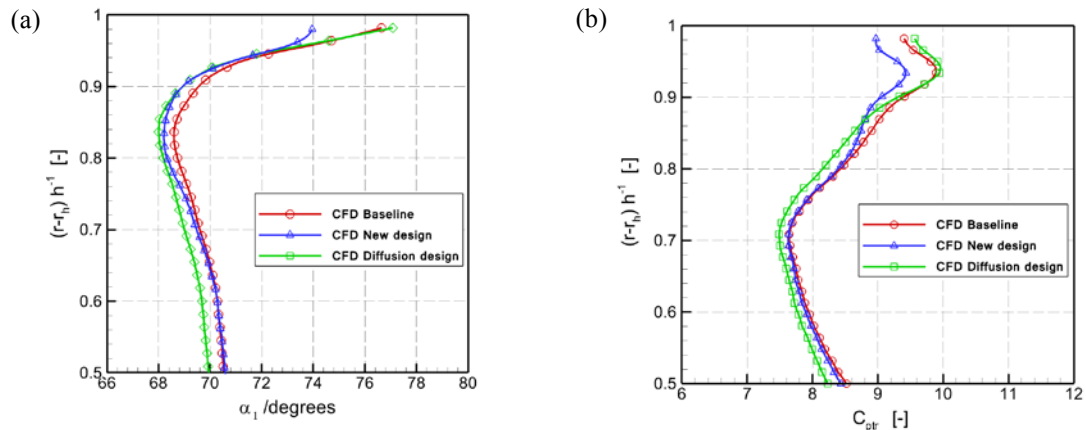


Fig. 5. Radial distributions of predicted pitch-averaged (a) yaw angle 8.8 mm downstream of the upstream stator exit plane and (b) total pressure loss coefficient 8.8 mm downstream of the rotor exit plane.

Fig. 5 (a-b) show the mid-span to casing radial distributions of the yaw angle  $\alpha_1$ , 8.8 mm downstream of the upstream stator exit, and of the pitch-averaged total pressure loss coefficient  $C_{ptr}$ , 8.8 mm downstream of the rotor exit.  $\alpha_1$  and  $C_{ptr}$  from the simulations are compared between the baseline, the casing of new design, and the casing with a diffusion design. The yaw angle distribution in Fig. 5 (a) shows over-turning above the design yaw angle of  $70^\circ$  near the casing. The new design for the casing mitigates this over-turning compared to both the baseline and the diffusion design. This results in a more spanwise uniform flow angle. Fig. 5 (b) shows that, as this overturning is reduced, the pitch mass-averaged total pressure loss is reduced near the casing, at the expense of a small additional loss further outbound. The diffusion design produces lower contributions to the total pressure loss coefficient from the midspan up to 0.88 span.

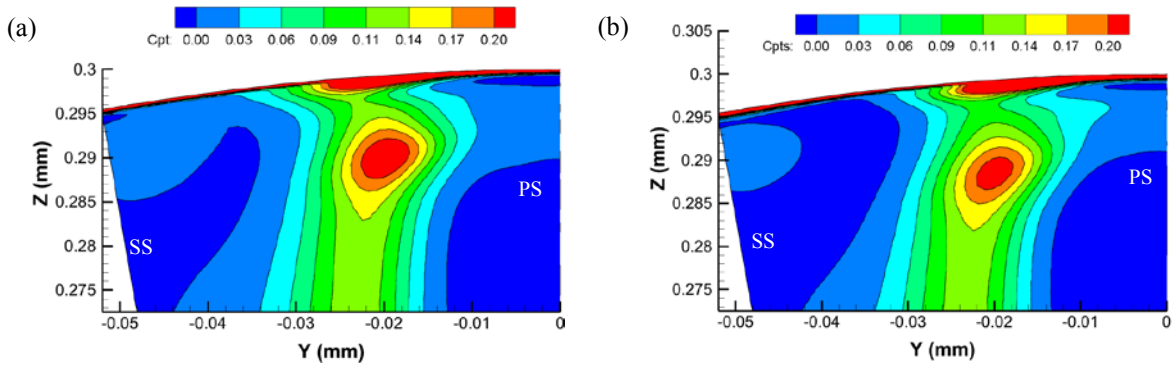


Fig. 6. Contours of total pressure loss coefficient at 8.8 mm behind the upstream stator off design: (a) axisymmetric casing, (b) contoured casing by the new design.

A further insight into the through-flow at off-design conditions is provided by Fig. 6, which presents the contours of the total pressure loss coefficient 8.8 mm behind the upstream stator with an axisymmetric and a contoured casing of new design. Fig. 6 shows a core of high total pressure loss coefficient, located approximately at  $Z = 0.291$  mm and  $Y = -0.019$  mm, which is reduced in extent by the contoured casing. The location of this maximum is consistent with that of the casing passage vortex (PV) in [10].

Fig. 7 shows the entropy distributions at the exit of the rotor passage with and without the contoured casing of new design. It shows that the entropy production caused by the tip leakage vortex appears to reduce by the use of the new contoured casing.

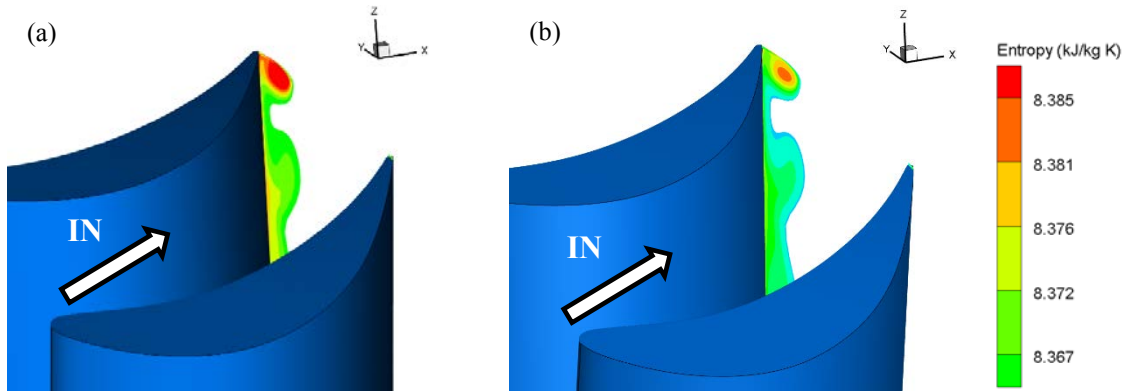


Fig. 7. Entropy distributions at the rotor exit off-design: (a) axisymmetric casing, (b) contoured casing of new design.

**5. Conclusions**

A newly designed casing end-wall was applied to improve the aerodynamic performance of a 1.5 stage axial turbine. Measurements from RWTH Aachen were used to validate a RANS  $k - \omega$  SST model of the Aachen Turbine and gave confidence in its use for studying the effect of the new casing on the flow. The current design produces aerodynamic performance gains at design and off design. There appears to have been a positive effect on the rotor tip leakage flow. Numerical predictions with the new contoured casing and with a contoured casing geometry from Sun et al. [11] indicate a more spanwise uniform outflow angle, which stands to benefit the downstream stator rows. The industry-wide adoption of this technology would have significant economic and environmental impacts.

**Acknowledgements**

This work was undertaken under the auspices of the GE – University of Leicester framework agreement. Advice

from Dr. N. Z. Ince and Dr. M. Willetts, GE, is gratefully acknowledged. The Higher Committee for Education Development in Iraq (HCED), is acknowledged. This research used the ALICE high performance computing facility at the University of Leicester. Graphical rendering software licenses were originally acquired with EPSRC support on Grant GR/N23745/01. The supply of experimental data for the 1.5 stage axial flow turbine “Aachen turbine” under license by RWTH Aachen is gratefully acknowledged.

## References

- [1] Schobeiri, M. Turbomachinery flow physics and dynamic performance, In, Springer, 2005.
- [2] Langston, L. Secondary flows in axial turbines—a review. *Annals of the New York Academy of Sciences*, 2001, 934(1) pp 11-26.
- [3] Kadhim, H. T., Rona, A. Perspectives on the Treatment of Secondary Flows in Axial Turbines. In: 9th International Conference on Applied Energy, ICAE, Elsevier Ltd., 2017.
- [4] Wang, H. P., Olson, S. J., Goldstein, R. J., Eckert, E. R. G. Flow Visualization in a Linear Turbine Cascade of High Performance Turbine Blades. *Journal of Turbomachinery*, 1997, 119(1) pp 1-8.
- [5] Sieverding, C. H. Recent Progress in the Understanding of Basic Aspects of Secondary Flows in Turbine Blade Passages. *Journal of Engineering for Gas Turbines and Power*, 1985, 107(2) pp 248-257.
- [6] Acharya, S., Mahmood, G. Turbine Blade Aerodynamics. *The Gas Turbine Handbook*, 2006, 1.
- [7] Gostelow, J. P., Mahallati, A., Carscallen, W., Rona, A. Encounters with vortices in a turbine nozzle passage. *International Journal of Rotating Machinery*, 2012, 2012.
- [8] Kadhim, H. T., Rona, A., Obaida, H. M., Gostelow, J. P. Numerical Study of the Flow past an Axial Turbine Stator Casing and Perspectives for Its Management. In: ASME Turbo Expo 2017: Turbine Technical Conference and Exposition, 2017, ASME Paper GT2107-63055.
- [9] Kadhim, H. T., Rona, A., Leschke, K., Gostelow, J. P. Mitigating Secondary Flows In a 1½ Stage Axial Turbine by Design a Guide Groove Casing. In: ISABE-2017, 2017, pp 1-10.
- [10] Gallus, H. E., Zeschky, J. Secondary Flow and Losses in a Turbine Rotor at Off-Design Conditions In: *Ciepłne Maszyny Przepływowe (CMP)*, 1992.
- [11] Sun, H., Li, J., Song, L., Feng, Z. Non-Axisymmetric Turbine Endwall Aerodynamic Optimization Design: Part I—Turbine Cascade Design and Experimental Validations. In: ASME Turbo Expo 2014: Turbine Technical Conference and Exposition, American Society of Mechanical Engineers, 2014, ASME Paper GT2014-25362.